



A commentary by Kanu Okike, MD, MPH, is linked to the online version of this article at jbjs.org.

Computer-Assisted Virtual Surgical Technology Versus Three-Dimensional Printing Technology in Preoperative Planning for Displaced Three and Four-Part Fractures of the Proximal End of the Humerus

Yanxi Chen, MD, PhD, Xiaoyang Jia, MD, Minfei Qiang, MD, Kun Zhang, MD, and Song Chen, MD

Investigation performed at the Department of Orthopedic Trauma, East Hospital, Tongji University School of Medicine, Shanghai, China

Background: This study aimed to determine the difference between computer-assisted virtual surgical technology and 3-dimensional (3D) printing technology in preoperative planning for proximal humeral fractures.

Methods: Between February 2009 and October 2015, 131 patients with 3 and 4-part proximal humeral fractures were divided into 3 groups on the basis of the preoperative planning method: conventional ($n = 53$), virtual surgical ($n = 46$), and 3D printing ($n = 32$). Fracture characteristics and intraoperative realization of preoperative planning (reduction shape and implant choices) were evaluated. Postoperative functional outcomes were assessed using the American Shoulder and Elbow Surgeons, Constant-Murley, and Short Form-36 (SF-36) scoring systems and shoulder range of motion; postoperative radiographic outcomes were assessed with respect to the loss of the neck-shaft angle (NSA) and loss of humeral head height (HHH).

Results: Excellent sensitivity, specificity, and accuracy for fracture characteristics were seen in all 3 groups. The correlations for NSA ($p = 0.033$) and HHH ($p = 0.035$) were higher in the virtual surgical group than in the 3D printing group. The lengths of the medial support screws in the actual choices were shorter than those in the preoperative plan for the 3D printing group, but a similar pattern was not seen in the virtual surgical group. Compared with the conventional method, the virtual surgical and 3D printing methods of preoperative planning resulted in shorter operative time, less blood loss, and fewer fluoroscopic images. The functional outcomes in both the 3D printing and virtual surgical groups were better than those in the conventional group. The virtual surgical method was faster than the 3D printing method, as suggested by a shorter time to surgery (2.5 compared with 4.6 days; $p < 0.001$), a shorter time for preoperative planning (30.4 compared with 262.4 minutes; $p < 0.001$), and a decreased duration of hospital stay (10.9 compared with 14.6 days; $p < 0.001$).

Conclusions: The clinical outcomes in both the virtual surgical and 3D printing groups were better than those in the conventional group. However, computer-assisted virtual surgical technology is more convenient and efficient, considering the shorter time for preoperative planning. In addition, it has improved correlation with preoperative planning.

Level of Evidence: Therapeutic Level III. See Instructions for Authors for a complete description of levels of evidence.

Fractures of the proximal end of the humerus are the second most common fractures of the upper extremity, accounting for approximately 10% of all fractures in patients

who are ≥ 65 years old^{1,2}. For displaced 3 and 4-part fractures, the outcomes of surgical management are unsatisfactory²⁻⁷. Inaccurate preoperative evaluation of fracture characteristics, incomplete

Disclosure: There was no external funding source for this study. The **Disclosure of Potential Conflicts of Interest** forms are provided with the online version of the article (<http://links.lww.com/JBJS/E978>).

intraoperative fracture reduction, and improper implant choices are associated with inadequate outcomes⁸⁻¹⁰. Therefore, effective preoperative planning is advocated, as it may improve the results of surgical management and minimize the risks associated with inappropriate management^{8,9,11-13}.

Three-dimensional (3D) printing technology and computer-assisted virtual surgical technology based on computed tomography (CT) post-processing have become the 2 main advanced methods of preoperative planning¹²⁻¹⁵. A 3D printing model provides a direct and interactive display of fracture characteristics for surgeons. In addition, it can be used to perform virtual procedures in vitro such as fracture reduction and simulation surgery, which is conducive to creating a complete preoperative plan^{8-11,16}. The operative time, intraoperative blood loss, and number of fluoroscopic images have been reported to decrease with use of 3D printing technology compared with conven-

tional surgery for complex pelvic and proximal humeral fractures^{8,9}. However, the procedures for printing, segmentation, and immobilization of the 3D model are time-consuming, tedious, and complex¹⁶. The use of computer-assisted virtual surgical technology enables multilevel and multiangle evaluation of fracture planes. Surgeons can perform the surgery virtually, including reducing the fracture fragments and selecting a suitable internal fixation device^{13,14}. In the past, the application of virtual surgery required clinicians to have basic knowledge of computer image processing. With further advances in computer technology, an efficient system for computer-assisted preoperative planning has been developed^{13,14}. To our knowledge, there is no evidence supporting one technology over another for preoperative planning in the treatment of complex fractures.

The aim of this study was to compare the differences between 3D printing technology and computer-assisted virtual

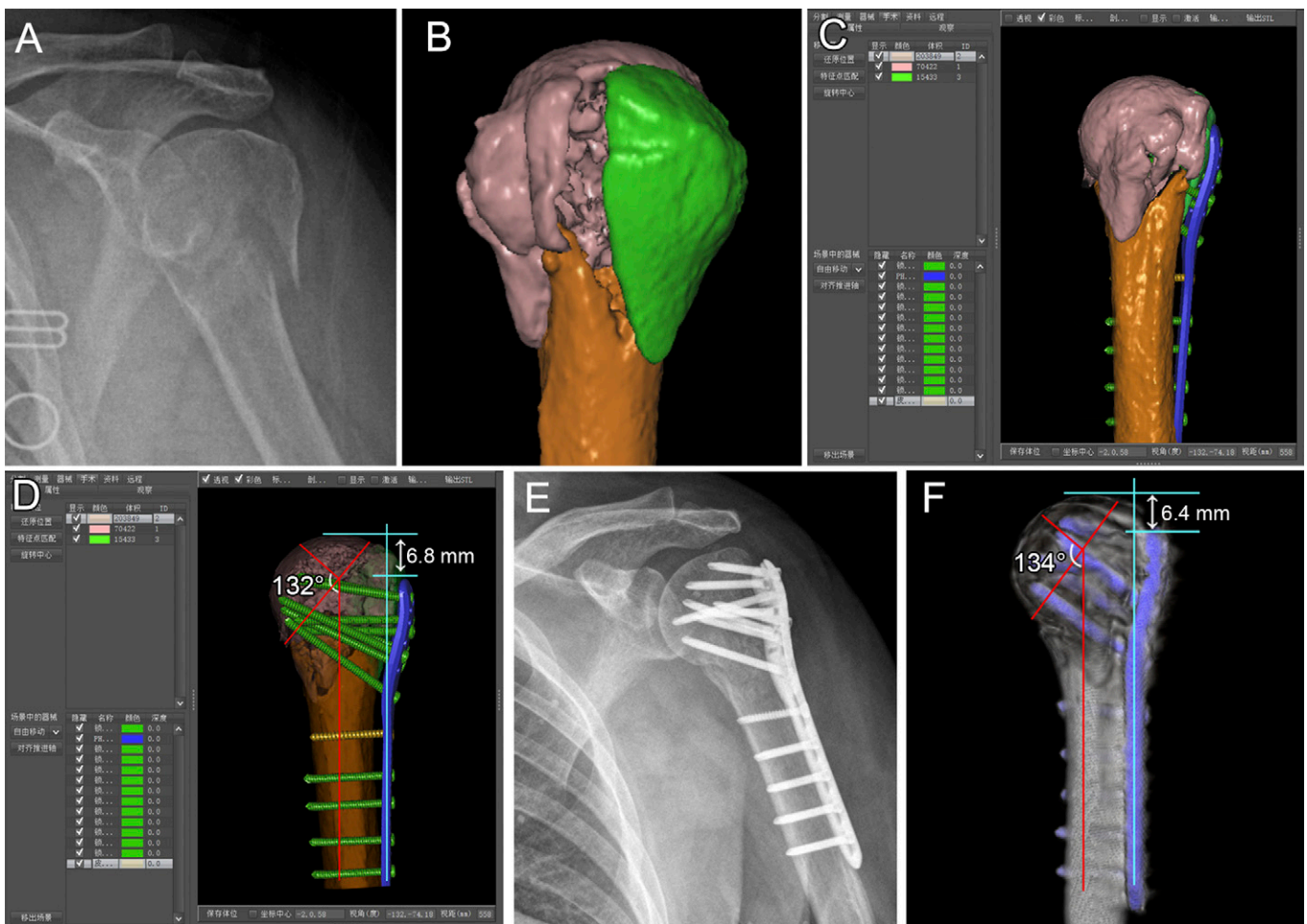


Fig. 1
Figs. 1-A through 1-F Application of computer-assisted virtual surgical technology in preoperative planning for fractures of the proximal end of the humerus. **Figs. 1-A and 1-B** Anteroposterior radiograph (**Fig. 1-A**) and 3D surface-shaded display image (**Fig. 1-B**) of a 78-year-old woman who fell off the bed and sustained a 3-part proximal humeral fracture. **Fig. 1-C** Proper internal fixation devices were placed after simulation of the fracture reduction. **Fig. 1-D** The NSA was 132°, and HHH (the vertical distance from the highest point of the plate to the highest point of the humeral head) was 6.8 mm. **Fig. 1-E** Postoperative radiograph showing the high consistency between the surgical procedure and the preoperative planning with use of computer-assisted virtual surgical technology. **Fig. 1-F** The NSA was 134° and HHH was 6.4 mm in the postoperative initial 3D image.

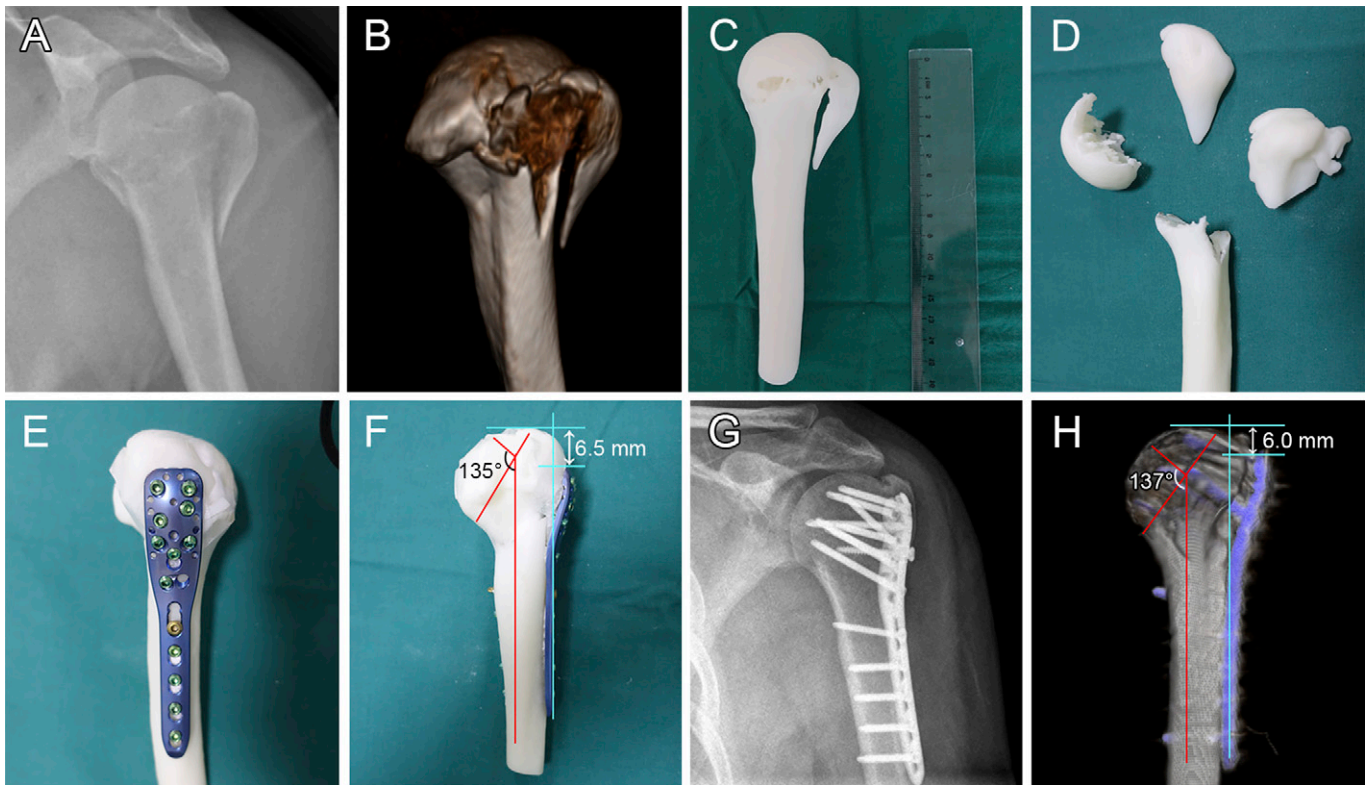


Fig. 2

Figs. 2-A through 2-H Application of 3D printing technology in preoperative planning for fractures of the proximal end of the humerus. **Figs. 2-A and 2-B** Anteroposterior radiograph (**Fig. 2-A**) and 3D volume rendering image (**Fig. 2-B**) of a 74-year-old woman who fell from a height and sustained a 4-part proximal humeral fracture. **Figs. 2-C and 2-D** The life-sized 3D model was printed (**Fig. 2-C**), and then it was segmented in the direction of the fracture line (**Fig. 2-D**). **Fig. 2-E** Appropriate internal fixation devices were placed after the simulation of fracture reduction. **Fig. 2-F** The NSA was 135°, and HHH (the vertical distance from the highest point of the plate to the highest point of the humeral head) was 6.5 mm. **Fig. 2-G** Postoperative radiograph showing the high consistency between the surgical procedure and the preoperative planning with use of 3D printing technology. **Fig. 2-H** The NSA was 137°, and HHH was 6.0 mm in the postoperative initial 3D image.

surgical technology for the accuracy of fracture characteristic identification, intraoperative completion of preoperative planning, and clinical outcomes for displaced 3 and 4-part fractures of the proximal end of the humerus.

Materials and Methods

Patients

We retrospectively reviewed the clinical and imaging data of patients with a complex fracture of the proximal end of the humerus who were treated with locking plates and open reduction and internal fixation. We searched medical records and a medical imaging database and identified 159 consecutive patients with such fractures who were treated from February 2009 to October 2015. Patients who had a 3 or 4-part fracture according to the Neer classification system¹⁷, an age of ≥ 18 years, an injury-to-surgery interval within 2 weeks, and no other injuries of the ipsilateral upper limb were included in this study. Those who had pathological fractures, open fractures, or neuromuscular injury were excluded. Of the 159 patients, 24 were excluded because of age and the interval between injury and surgery, 2 patients declined to accept the assigned reha-

bilitation algorithm, and 2 patients were lost to follow-up. Therefore, 131 patients with a fracture of the proximal end of the humerus (35 men and 96 women) and a mean age of 70.2 years (range, 43 to 89 years) constituted the study population. The institutional review board approved this study, and written informed consent was obtained.

All patients had radiographs of the injured shoulder made preoperatively and at each follow-up visit. Follow-up was conducted at 3, 6, and 12 months postoperatively and yearly thereafter. CT scans were performed preoperatively and at 12 months postoperatively. All CT images were obtained using a 16-detector spiral CT scanner (GE LightSpeed CT).

Preoperative Evaluation and Planning

The preoperative planning for conventional and computer-assisted virtual surgical groups was performed in the clinical setting from February 2009 to May 2013, and 3D printing was added to the preoperative planning between June 2013 and October 2015. Therefore, patients were divided into 3 groups: conventional, virtual surgical, and 3D printing groups. All preoperative plans were conducted by the senior author (Y.C.).

TABLE I Patient Demographics and Fracture Characteristics *

	Conventional Group (N = 53)	3D Printing Group (N = 32)	Virtual Surgical Group (N = 46)	P Value
Sex†				0.897
Male	13 (24.5)	9 (28.1)	13 (28.3)	
Female	40 (75.5)	23 (71.9)	33 (71.7)	
Age‡ (yr)	70.0 (43-89)	69.5 (49-86)	70.9 (47-85)	0.699
BMI§ (kg/m ²)	24.5 ± 0.9	24.7 ± 1.4	24.6 ± 1.2	0.787
Education†				0.946
Primary school	31 (58.5)	20 (62.5)	26 (56.5)	
Junior high school	16 (30.2)	10 (31.3)	15 (32.6)	
Senior high school or above	6 (11.3)	2 (6.3)	5 (10.9)	
Diabetes†	6 (11.3)	5 (15.6)	6 (13.0)	0.849
Smoking status†	3 (5.7)	2 (6.3)	4 (8.7)	0.827
Steroid use†	4 (7.5)	3 (9.4)	3 (6.5)	0.896
Injury mechanism†				0.998
Falling from height	36 (67.9)	22 (68.8)	32 (69.6)	
Traffic accident	15 (28.3)	9 (28.1)	12 (36.1)	
Other	2 (3.8)	1 (3.1)	2 (4.3)	
Neer classification†				0.725
3-part	33 (62.3)	19 (59.4)	25 (54.3)	
4-part	20 (37.7)	13 (40.6)	21 (45.7)	
Affected shoulder†				0.626
Left	29 (54.7)	15 (46.9)	21 (45.7)	
Right	24 (45.3)	17 (53.1)	25 (54.3)	
Dominant side†	26 (49.1)	18 (56.3)	26 (56.5)	0.709
Injury-surgery interval§ (days)	2.8 ± 1.0	4.6 ± 1.2	2.5 ± 1.0	<0.001#
Surgical approach†				0.912
Deltopectoral	24 (45.3)	16 (50.0)	22 (47.8)	
Deltoid-splitting	29 (54.7)	16 (50.0)	24 (52.2)	

*BMI = body mass index. †The values are given as the number, with the percentage in parentheses. ‡The values are given as the mean, with the range in parentheses. §The values are given as the mean and the standard deviation. #There was a significant difference among the 3 groups ($p < 0.001$ for conventional versus 3D printing, $p = 0.28$ for conventional versus virtual surgical, and $p < 0.001$ for 3D printing versus virtual surgical).

In the conventional group, preoperative planning was based on radiography and CT images (including 2-dimensional [2D] and 3D imaging) in combination with the surgeon's experience, which was the regular method for most orthopaedic surgeons.

In the virtual surgical group, the CT images were entered into the computer-aided orthopaedic clinical research platform (SuperImage orthopaedic edition 1.1; Cybermed)¹⁸. A 3D image of the proximal humeral fracture was reconstructed using a surface-shaded display algorithm, and fracture fragments were marked with distinct colors (Fig. 1). Reduction of the fractures was simulated (see Appendix), and then the suitable proximal humeral internal locking system (PHILOS) plate (DePuy Synthes) and an appropriate length of 3.5-mm-diameter screws were chosen (Fig. 1).

In the 3D printing group, the 3D reconstructive model was stored in the stereolithography format, which was subsequently

transferred to a 3D printer (JGAurora Z-603S; JGAurora Technology). A life-sized 3D model was obtained, and then the model of the fracture was segmented (Fig. 2). Proper fracture reduction was achieved and maintained using glue. The suitable PHILOS plate and screws were selected (Fig. 2).

Before simulation surgery, 2 senior orthopaedic surgeons (Y.C. and M.Q.), using the images and 3D model (only images for the conventional and virtual group, and images combined with the 3D model for the 3D printing group), were required to answer 4 questions for each fracture: (1) Is the greater tuberosity displaced? (2) Is the humeral head split? (3) Is the arterial supply compromised?¹⁹ and (4) What is the classification of the fracture: 3-part or 4-part?¹⁷

Operative Technique

All surgical procedures were performed by the senior surgeon (Y.C.), who had 18 years of clinical experience in treating fractures

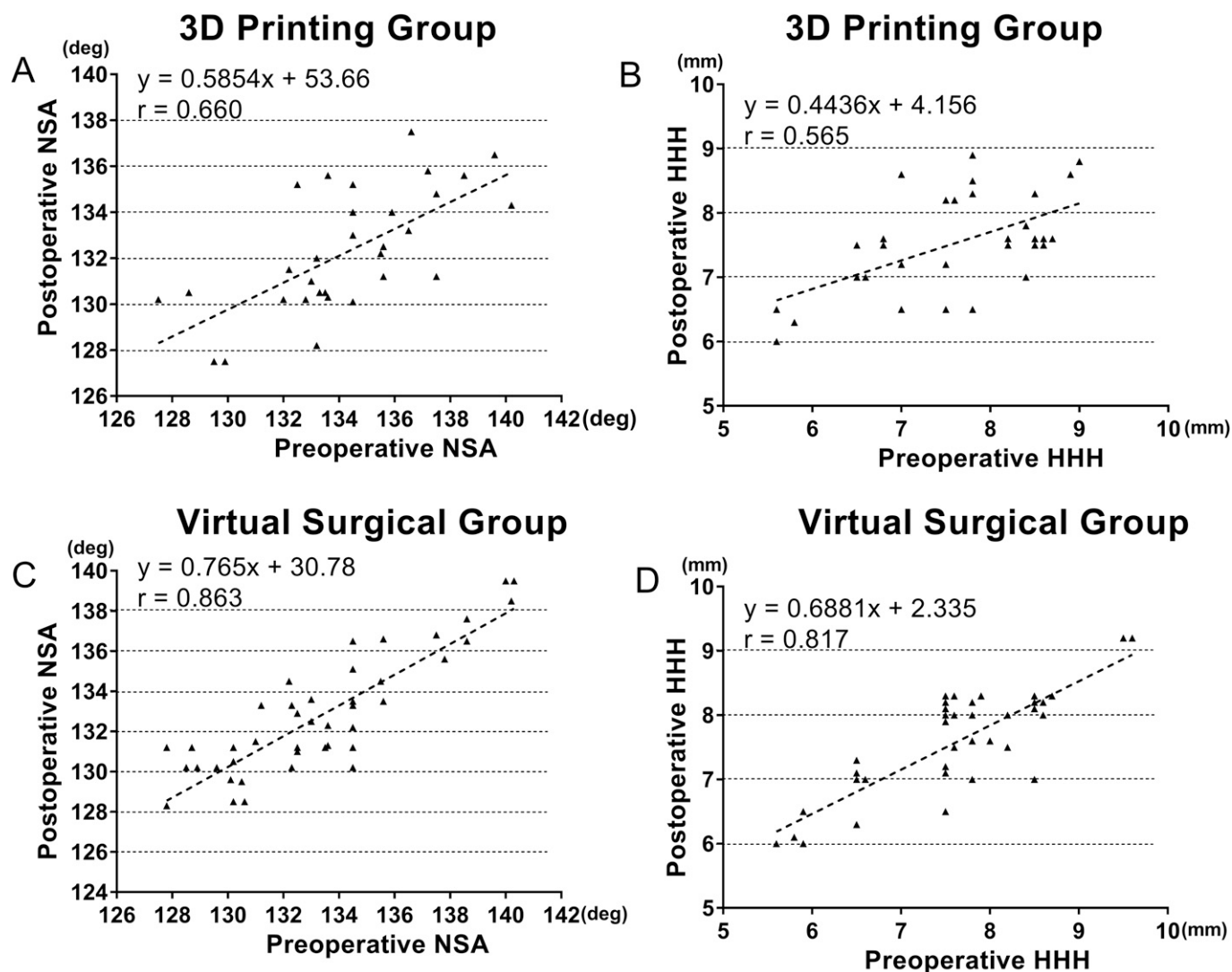


Fig. 3

Figs. 3-A through 3-D Correlations between the preoperative plan and images on postoperative day 1; fracture reduction was assessed by measuring the NSA and HHH in the 3D printing group (**Figs. 3-A and 3-B**, respectively) and the virtual surgical group (**Figs. 3-C and 3-D**). Correlation of NSA values was 0.660 in the 3D printing group (**Fig. 3-A**) and 0.863 in the virtual surgical group (**Fig. 3-C**) ($p = 0.033$). Correlation of HHH values was 0.565 in the 3D printing group (**Fig. 3-B**) and 0.817 in the virtual surgical group (**Fig. 3-D**) ($p = 0.035$).

of the proximal aspect of the humerus. Fracture reduction and suitable internal fixation were determined with preoperative planning and intraoperative fluoroscopy.

Evaluation

To evaluate the accuracy of preoperative plans, preoperative planning and postoperative reduction (postoperative day 1) were compared with respect to neck-shaft angle (NSA) and humeral head height (HHH)^{20,21}. The postoperative day 1 radiographs were reviewed by 1 of the authors (X.J.), who was blinded as to which planning group the patient was from. The screw holes in the plates were numbered from 1 to 9 for the proximal end and from 1 to 6 for the distal end (there were 3 distal holes in a small plate, 5 distal holes in a medium plate, and 6 distal holes in a large plate) (see Appendix).

The functional outcomes were evaluated at the time of the 24-month follow-up with the American Shoulder and Elbow Surgeons (ASES), Constant-Murley, and Short Form-36 (SF-36) physical component summary (PCS) scoring systems and range of motion (including forward flexion, abduction, and external rotation). The SF-36 PCS outcome was normalized to a 100-point scale ($[\text{score} - 10] \times 100/20$). The radiographic outcomes were the loss of NSA and loss of HHH between postoperative day 1 and month 12 (loss = day 1 – month 12).

Statistical Analysis

The so-called gold standard method was based on the surgeon's intraoperative observation for the 4 fracture characteristics. The sensitivity, specificity, and accuracy of the fracture characteristics were calculated for each observer, and the values

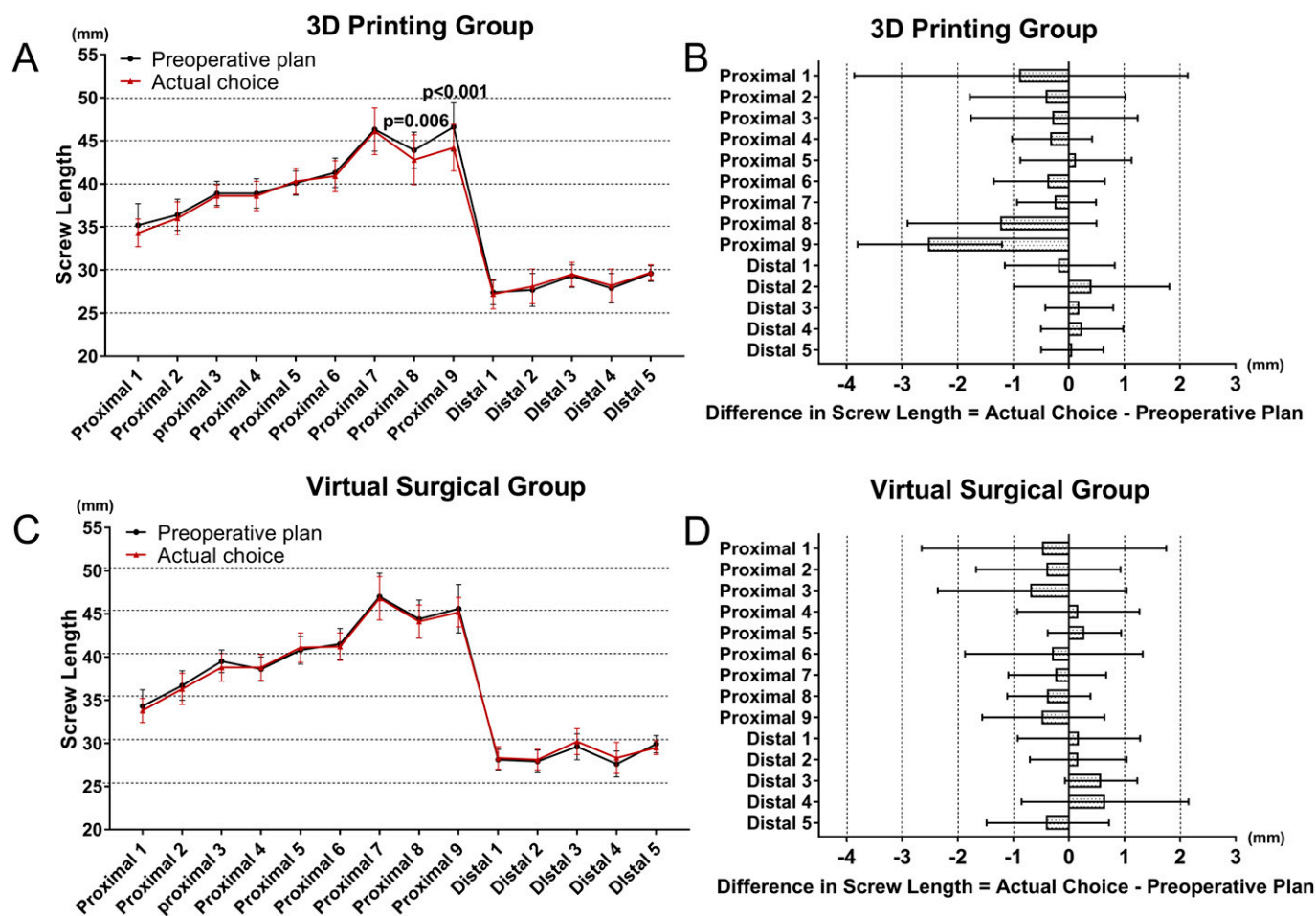


Fig. 4

Figs. 4-A through 4-D Screw choices in the 3D printing group (**Figs. 4-A and 4-B**) and the virtual surgical group (**Figs. 4-C and 4-D**). The error bars represent the standard deviation. The average lengths of screws in the preoperative plan are compared with the actual choices in the 3D printing group (**Fig. 4-A**) and virtual surgical group (**Fig. 4-C**). The differences between the preoperative plan and the actual choice in the 3D printing group (**Fig. 4-B**) and the virtual surgical group (**Fig. 4-D**) are also depicted. Shorter screws were chosen in the operation for the proximal screw holes 8 and 9 (medial support screws) compared with the preoperative plan in the 3D printing group, but not in the virtual surgical group (**Figs. 4-A and 4-C**).

were averaged. The accuracy of fracture reduction was determined with the Pearson correlation coefficient (r). Two-sample independent Z tests were performed for the accuracy of fracture characteristics and reduction. To compare the screw lengths between preoperative planning and the actual choice, the paired t test was used. The independent sample t test was performed to compare the time needed for preoperative planning between the 3D printing and virtual surgical groups. Differences among multiple groups were tested with analysis of variance, and if necessary, the least significant difference t test would be used. Categorical data were compared with the chi-square or Fisher exact test, and if necessary, partition of chi-square was used. Age, body mass index, and fracture classification are potential confounding factors for postoperative outcomes²². Therefore, multivariate linear regression analysis was performed to compare the difference among the 3 groups for functional and radiographic outcomes, and logistic regression analysis was used for comparing the postoperative

complication rate with adjustment for the 3 potential confounding factors. Significance was defined as $p < 0.05$. Statistical analysis was performed with SPSS software (version 19.0; IBM).

Results

Clinical Data

Of 131 patients, 53 (40.4%) were in the conventional group; 32 (24.4%), in the 3D printing group; and 46 (35.1%), in the virtual surgical group. The demographic and baseline characteristics are shown in Table I. The mean follow-up period was 26.2 months (range, 24 to 33 months) in the conventional group, 26.6 months (range, 24 to 30 months) in the 3D printing group, and 26.7 months (range, 24 to 33 months) in the virtual surgical group ($p = 0.307$). The mean time from injury to surgery was longer in the 3D printing group (range, 2 to 6 days) than in the conventional (range, 0 to 7 days; $p < 0.001$) and virtual surgical groups (range, 0 to 7 days; $p < 0.001$) (Table I).

TABLE II Clinical Outcomes in Different Groups*

	Conventional Group (N = 53)	3D Printing Group (N = 32)	Virtual Surgical Group (N = 46)	P Value		
				Conventional Vs. 3D Printing	Conventional Vs. Virtual Surgical	3D Printing Vs. Virtual Surgical
Preop. planning time† (min)	NA	262.4 ± 18.3	30.4 ± 4.6	NA	NA	<0.001
Operative time† (min)	80.4 ± 8.9	61.5 ± 9.3	62.7 ± 8.0	<0.001	<0.001	0.551
Intraop. blood loss† (mL)	100.5 ± 12.5	83.1 ± 13.0	82.2 ± 7.2	<0.001	<0.001	0.731
No. of fluoroscopies†	8.3 ± 1.4	5.7 ± 1.1	6.1 ± 1.4	<0.001	<0.001	0.198
Duration of hospital stay† (days)	11.1 ± 1.8	14.6 ± 1.6	10.9 ± 1.8	<0.001	0.563	<0.001
Complication rate (no. [%])	5 (9.4)	4 (12.5)	1 (2.2)	0.656	0.155	0.096
Loss of NSA† (deg)	5.0 ± 1.8	5.5 ± 2.1	5.6 ± 1.8	0.242	0.070	0.649
Loss of HHH† (mm)	2.6 ± 1.3	3.0 ± 1.0	2.7 ± 1.1	0.138	0.624	0.310
ASES score† (points)	68.5 ± 5.6	75.0 ± 6.3	75.1 ± 3.4	<0.001	<0.001	0.977
Constant score† (points)	66.9 ± 3.6	73.9 ± 4.4	73.3 ± 5.0	<0.001	<0.001	0.490
Range of motion† (deg)						
Forward flexion	136.3 ± 9.8	157.0 ± 10.1	155.2 ± 8.8	<0.001	<0.001	0.369
Abduction	95.6 ± 11.0	126.0 ± 11.3	127.7 ± 12.3	<0.001	<0.001	0.529
External rotation	38.4 ± 9.6	48.1 ± 10.8	47.1 ± 7.2	<0.001	<0.001	0.488
SF-36 PCS† (points)	70.2 ± 3.3	75.1 ± 7.0	74.9 ± 2.8	<0.001	<0.001	0.916

*NA = not applicable, NSA = neck-shaft angle, and HHH = humeral head height. †The values are given as the mean and the standard deviation.

Accuracy of Preoperative Evaluation and Planning

The accuracy of determining the existence of a fracture of the greater tuberosity was 0.92 in the conventional group, 0.88 in the 3D printing group, and 0.87 in the virtual surgical group ($p = 0.41$ for the conventional group versus the 3D printing group, $p = 0.33$ for the conventional group versus the virtual surgical group, and $p = 0.99$ for the 3D printing group versus the virtual surgical group). Excellent sensitivity and specificity for fractures of the greater tuberosity were seen in all 3 groups. Comparable results were observed for splitting of the humeral head, compromise of the arterial supply, and fracture classification (see Appendix).

Good correlation between preoperative planning and postoperative day 1 was seen for NSA ($r = 0.660$ in the 3D printing group, and $r = 0.863$ in the virtual surgical group) and HHH ($r = 0.565$ in the 3D printing group and $r = 0.817$ in the virtual surgical group) (Fig. 3). The correlations for NSA ($p = 0.033$) and HHH ($p = 0.035$) were higher in the virtual surgical group than in the 3D printing group.

The planned size of plate was used in all the actual operations. The numbers of screws in the preoperative plan were consistent with those in the actual choice for both the 3D printing and virtual surgical groups. The length of screws and the differences between the preoperative plan and actual choice for screw length are shown in Figure 4. In the 3D printing group, the lengths of screws for the proximal screw holes 8 and 9 in the actual choice were shorter than those in the preoperative plan ($p < 0.05$ for both) (Fig. 4).

Functional and Radiographic Outcomes

A shorter time of preoperative planning was seen in the virtual surgical group (range, 22 to 45 minutes) than in the 3D printing group (range, 214 to 290 min) ($p < 0.001$) (Table II). Shorter operative time, less blood loss, and fewer fluoroscopic images were seen in the 3D printing and virtual surgical groups than in the conventional group ($p < 0.001$ for all) (Table II). Patients in the 3D printing group had a longer hospital stay than those in the conventional and virtual surgical groups ($p < 0.001$ for both) (Table II). Higher ASES scores were found in the 3D printing (95% confidence interval [CI], 72.7 to 77.2) and virtual surgical groups (95% CI, 74.1 to 76.1) than in the conventional group (95% CI, 66.9 to 70.2) ($p < 0.001$ for both) (Table II). Comparable results were observed for the Constant score, SF-36 PCS score, and range of motion of the injured shoulder (Table II). However, there was no significant difference among the 3 groups with regard to the loss of NSA and HHH (Table II).

Complications

Three patients (2 in the conventional group and 1 in the 3D printing group) had screw penetration, and implants were removed after 1 year (Table II). Five patients (2 in the conventional group, 2 in the 3D printing group, and 1 in the virtual surgical group) had a superficial infection that healed with local wound treatment and oral antibiotics (Table II). Two patients (1 in the conventional group and 1 in the 3D printing group) had implant failure, and they underwent a second operation (Table II). There was no significant difference

among the 3 groups with regard to postoperative complication rate (Table II).

Discussion

This study aimed to determine whether there is a difference between 3D printing technology and computer-assisted virtual surgical technology in terms of the accuracy of fracture characteristics, intraoperative realization of preoperative planning, and clinical outcomes for complex proximal humeral fractures. In this study, good sensitivity, specificity, and accuracy of fracture characteristics were obtained in all 3 groups. Better accuracy in terms of fracture reduction and implant choice was found in the virtual surgical group. Although similar clinical outcomes were seen between the virtual surgical and 3D printing groups, there were some advantages of the virtual surgical technology in terms of shorter time of preoperative planning, interval from injury to surgery, and duration of hospital stay.

Patients in the virtual surgical and 3D printing groups had a shorter operative time, less blood loss, fewer fluoroscopic images, and better functional outcomes than those in the conventional group. The advantage may have resulted from the fact that the reconstructive process allows more detailed observation and intuitive understanding of fracture characteristics for surgeons^{8-10,14}. This enables surgeons to confirm the fracture details, determine the morphology of the fracture line and the number and position of fragments, examine the collapse and comminuted condition of the articular surface, verify the potential presence of bone defects, and determine whether a bone graft is needed. Additionally, appropriate internal implants were obtained on the basis of the simulation surgery. These processes were conducive for restoring the fragments accurately and selecting proper internal implants intraoperatively.

Computer-assisted virtual surgical and 3D printing technologies both can help surgeons to make an individual, accurate, and reasonable surgical plan for patients. However, virtual surgical technology had some advantages over 3D printing technology regarding the shorter time for preoperative planning, interval from injury to surgery, and duration of hospital stay. The procedures for surgical planning based on 3D printing technology required more time as they consisted of 3 steps. First, 3D images were reconstructed in the work platform and were sent to the 3D printer. Second, the 3D model was printed and carried to the surgeons. This process is time-consuming¹⁶, and it took a total of approximately 30 hours in this study. Finally, the model was segmented and repositioned, and the simulation surgery was conducted, which required an average of 4.5 hours in the present study. To our knowledge, there was no specific and effective tool to separate fracture fragments, and cutting knives were used in this study. The 3D-printed model is made of dense material, and it is hard to cut. In contrast, the 3D interactive and automatic segmentation technique was applied to segment the fracture fragments in the virtual surgical group¹³. The surgical planning took approximately half an hour with use of computer-assisted virtual surgical technology.

Some investigators have documented the costs associated with preoperative planning. Conventional preoperative planning was the standard method in the clinical setting, which did

not produce extra cost²³. Preoperative planning in the virtual surgical group was performed using a computer-aided orthopaedic clinical research platform developed by our research team. Therefore, no extra cost was incurred for the patients. Certain additional cost was incurred in the process of 3D printing but was borne by our research team. Therefore, it did not increase patient treatment costs.

Some limitations of this study should be noted. First, surgical simulation was performed in a situation without soft tissues so that the screws could be placed in any direction. Therefore, such elements during the actual surgery must be considered before performing a surgical procedure. Second, there was potential for selection bias as the study was retrospective. Therefore, the effects of potential confounding factors were statistically adjusted for. Although this approach can reduce bias to a certain extent, further research must be done in a larger randomized prospective study. Additionally, our hospital system's duration of stay may not relate to other treatment environments worldwide.

In conclusion, patients had better clinical outcomes in the virtual surgical and 3D printing groups than in the conventional group. It is more convenient and efficient to use computer-assisted virtual surgical technology, which can shorten the interval from injury to surgery, time of preoperative planning, and duration of hospital stay. In addition, this method shows better results for intraoperative achievement of preoperative planning. The results in this study provide a reference for clinicians to select a rational preoperative plan for complex fractures of the proximal aspect of the humerus.

Appendix

eA Figures showing the process of fracture reduction in preoperative planning with use of the computer-assisted virtual surgical technology and demonstrating the distribution of the screw holes of the PHILOS plate as well as a table showing the sensitivity, specificity, and accuracy of the fracture characteristics on the basis of the different preoperative planning techniques are available with online version of this article as a data supplement at [jbjs.org \(http://links.lww.com/JBJS/E979\)](http://links.lww.com/JBJS/E979). ■

Yanxi Chen, MD, PhD¹
Xiaoyang Jia, MD¹
Minfei Qiang, MD¹
Kun Zhang, MD¹
Song Chen, MD¹

¹Department of Orthopedic Trauma, East Hospital, Tongji University School of Medicine, Shanghai, China

E-mail address for Y. Chen: cyxtongji@126.com

ORCID iD for Y. Chen: [0000-0002-4021-6020](https://orcid.org/0000-0002-4021-6020)
ORCID iD for X. Jia: [0000-0002-6238-7947](https://orcid.org/0000-0002-6238-7947)
ORCID iD for M. Qiang: [0000-0001-7442-4787](https://orcid.org/0000-0001-7442-4787)
ORCID iD for K. Zhang: [0000-0003-1236-6299](https://orcid.org/0000-0003-1236-6299)
ORCID iD for S. Chen: [0000-0002-2505-7930](https://orcid.org/0000-0002-2505-7930)

References

1. Court-Brown CM, Caesar B. Epidemiology of adult fractures: a review. *Injury*. 2006 Aug;37(8):691-7. Epub 2006 Jun 30.
2. Bell JE, Leung BC, Spratt KF, Koval KJ, Weinstein JD, Goodman DC, Tosteson AN. Trends and variation in incidence, surgical treatment, and repeat surgery of proximal humeral fractures in the elderly. *J Bone Joint Surg Am*. 2011 Jan 19; 93(2):121-31.
3. Schlegel TF, Hawkins RJ. Displaced proximal humeral fractures: evaluation and treatment. *J Am Acad Orthop Surg*. 1994 Jan;2(1):54-78.
4. Olerud P, Ahrengart L, Ponzer S, Saving J, Tidermark J. Internal fixation versus nonoperative treatment of displaced 3-part proximal humeral fractures in elderly patients: a randomized controlled trial. *J Shoulder Elbow Surg*. 2011 Jul;20(5): 747-55. Epub 2011 Mar 24.
5. Fjalestad T, Hole MØ, Hovden IA, Blücher J, Strømsøe K. Surgical treatment with an angular stable plate for complex displaced proximal humeral fractures in elderly patients: a randomized controlled trial. *J Orthop Trauma*. 2012 Feb;26(2):98-106.
6. Agel J, Jones CB, Sanzone AG, Camuso M, Henley MB. Treatment of proximal humeral fractures with Polarus nail fixation. *J Shoulder Elbow Surg*. 2004 Mar-Apr; 13(2):191-5.
7. Rajasekhar C, Ray PS, Bhamra MS. Fixation of proximal humeral fractures with the Polarus nail. *J Shoulder Elbow Surg*. 2001 Jan-Feb;10(1):7-10.
8. Zeng C, Xing W, Wu Z, Huang H, Huang W. A combination of three-dimensional printing and computer-assisted virtual surgical procedure for preoperative planning of acetabular fracture reduction. *Injury*. 2016 Oct;47(10):2223-7. Epub 2016 Mar 17.
9. You W, Liu LJ, Chen HX, Xiong JY, Wang DM, Huang JH, Ding JL, Wang DP. Application of 3D printing technology on the treatment of complex proximal humeral fractures (Neer 3-part and 4-part) in old people. *Orthop Traumatol Surg Res*. 2016 Nov;102(7):897-903. Epub 2016 Aug 9.
10. Lou Y, Cai L, Wang C, Tang Q, Pan T, Guo X, Wang J. Comparison of traditional surgery and surgery assisted by three dimensional printing technology in the treatment of tibial plateau fractures. *Int Orthop*. 2017 Sep;41(9):1875-80. Epub 2017 Apr 10.
11. Victor J, Premanathan A. Virtual 3D planning and patient specific surgical guides for osteotomies around the knee: a feasibility and proof-of-concept study. *Bone Joint J*. 2013 Nov;95-B(11)(Suppl A):153-8.
12. Khan FA, Lipman JD, Pearle AD, Boland PJ, Healey JH. Surgical technique: computer-generated custom jigs improve accuracy of wide resection of bone tumors. *Clin Orthop Relat Res*. 2013 Jun;471(6):2007-16. Epub 2013 Jan 5.
13. Chen Y, Qiang M, Zhang K, Li H, Dai H. Novel computer-assisted preoperative planning system for humeral shaft fractures: report of 43 cases. *Int J Med Robot*. 2015 Jun;11(2):109-19. Epub 2014 Aug 22.
14. Yoshii Y, Kusakabe T, Akita K, Tung WL, Ishii T. Reproducibility of three dimensional digital preoperative planning for the osteosynthesis of distal radius fractures. *J Orthop Res*. 2017 Dec;35(12):2646-51. Epub 2017 May 2.
15. Brown GA, Firoozbakhsh K, DeCoster TA, Reyna JR Jr, Moneim M. Rapid prototyping: the future of trauma surgery? *J Bone Joint Surg Am*. 2003;85(Suppl 4): 49-55.
16. Mitsouras D, Liacouras P, Imanzadeh A, Giannopoulos AA, Cai T, Kumamaru KK, George E, Wake N, Caterson EJ, Pomahac B, Ho VB, Grant GT, Rybicki FJ. Medical 3D printing for the radiologist. *Radiographics*. 2015 Nov-Dec;35(7): 1965-88.
17. Neer CS 2nd. Four-segment classification of proximal humeral fractures: purpose and reliable use. *J Shoulder Elbow Surg*. 2002 Jul-Aug;11(4):389-400.
18. Jia XY, Chen YX, Qiang MF, Zhang K, Li HB, Jiang YC, Zhang YJ. Postoperative evaluation of reduction loss in proximal humeral fractures: a comparison of plain radiographs and computed tomography. *Orthop Surg*. 2017 May;9(2):167-73. Epub 2017 May 30.
19. Hertel R, Hempfing A, Stiehler M, Leunig M. Predictors of humeral head ischemia after intracapsular fracture of the proximal humerus. *J Shoulder Elbow Surg*. 2004 Jul-Aug;13(4):427-33.
20. Hertel R, Knothe U, Ballmer FT. Geometry of the proximal humerus and implications for prosthetic design. *J Shoulder Elbow Surg*. 2002 Jul-Aug;11(4):331-8.
21. Gardner MJ, Weil Y, Barker JU, Kelly BT, Helfet DL, Lorch DG. The importance of medial support in locked plating of proximal humerus fractures. *J Orthop Trauma*. 2007 Mar;21(3):185-91.
22. Owsley KC, Gorczyca JT. Fracture displacement and screw cutout after open reduction and locked plate fixation of proximal humeral fractures [corrected]. *J Bone Joint Surg Am*. 2008 Feb;90(2):233-40.
23. Hak DJ, Rose J, Stahel PF. Preoperative planning in orthopedic trauma: benefits and contemporary uses. *Orthopedics*. 2010 Aug;33(8):581-4.